PHYSICAL REVIEW B **67**, 020401(R) (2003)

# Spin-polarized scanning tunneling microscopy study of 360° walls in an external magnetic field

A. Kubetzka,* O. Pietzsch, M. Bode, and R. Wiesendanger
*Institute of Applied Physics and Microstructure Research Center, University of Hamburg, Jungiusstrasse 11, 20355 Hamburg, Germany*
(Received 4 September 2002; published 9 January 2003)

Spin-polarized scanning tunneling microscopy is employed to study the internal structure of 360° magnetic domain walls in ultrathin Fe nanowires prepared on W(110). They are formed by pairs of winding 180° walls in an increasing external magnetic field. Their width is governed by an equilibrium of exchange and Zeeman energy. In the relevant field range ($B \geqslant 50$ mT) the demagnetizing energy contributes only indirectly via an increased wall width, i.e., a reduced effective anisotropy, and nonlocal effects are negligible.

DOI: 10.1103/PhysRevB.67.020401 PACS number(s): 75.60.Ch, 07.79.Cz

## I. INTRODUCTION

The formation and stability of 360° domain walls plays a crucial role in remagnetization processes of thin ferromagnetic films with possible implications for the performance and development of magnetoresistive and magnetic random access memory devices.[1] They are formed in external fields applied along the easy direction of the magnetic material when pairs of 180° walls with the same sense of rotation are forced together. Their stability against a remagnetization into the uniform state is a manifestation of a hard axis anisotropy perpendicular to the rotational plane of the wall.[2,3] This anisotropy may be of crystalline origin or—in films with an in-plane magnetic easy direction—due to the shape anisotropy.[4]

In general, in the equilibrium state the Zeeman energy is balanced by a repulsion of the two walls due to both exchange and demagnetizing (or dipolar) energy. It has been shown theoretically within an effective one-dimensional (1D) model[3] that the dipolar energy can be neglected in the 1D case (spin chain), and that exchange repulsion should also be observable experimentally in the 2D case, but only for sufficiently thin films and small domain-wall separations.

In this work we employ spin-polarized scanning tunneling microscopy (SPSTM) to measure the evolution of 360° domain-wall profiles in two-atomic-layer-thick Fe nanowires in an increasing external field of $B = 50$–$800$ mT. We will show that in this field range nonlocal demagnetizing effects are negligible, and that the system is well described by a balance of exchange and Zeeman energy within a simple 1D model.

## II. EXPERIMENTAL DETAILS

The experiments were performed in a UHV system with different chambers for surface analysis, sample preparation, metal-vapor deposition, and cryogenic STM,[5] at a base pressure in the $10^{-11}$ mbar range. As a substrate, we used a W(110) single crystal with an average terrace width of $\approx 25$ nm. It was cleaned by repeated cycles of heating at $T = 1500$ K in an oxygen atmosphere of $5 \times 10^{-7}$ mbar and subsequent flashing at 2300 K. We deposited 1.8 monolayers (ML) of Fe at an elevated temperature of $T = 500 \pm 50$ K, where step-flow growth leads to a system of Fe nanowires with alternating monolayer and double layer (DL) coverage, extending along the substrate's step edges.[6,7] The W tip was etched *ex situ*, flashed *in vacuo* at $T = 2300$ K, and coated with a ferromagnetic film leading to a strong in-plane magnetic contrast.

With both tip and sample held at $T = 14$ K, maps of the differential conductance $dI/dU$ ("magnetic signal") were recorded simultaneously to the constant-current images (topography) by adding a modulation voltage of $U_{\mathrm{mod}} = 10\ \mathrm{mV_{rms}}$ to the sample bias $U$ and detecting the $dI/dU$ signal by lock-in technique in closed feedback circuit configuration.

## III. RESULTS AND DISCUSSION

Fe DL nanowires on W(110) have a perpendicular magnetic easy axis and exhibit a transition from dipolar antiparallel coupling[7,6] to dense stripe domains with the coverage approaching 2.0 ML.[8]

Figure 1 displays the sample's topography and magnetic initial state as a 3D composite for $\Theta = 1.8$ ML. Within the

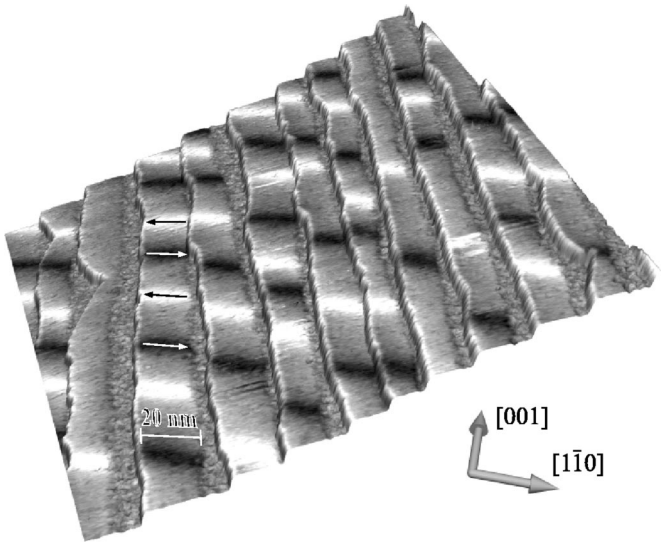


FIG. 1. $200 \times 200$ nm$^2$ constant-current (topography) image of 1.8 ML Fe on W(110), colorized with $dI/dU$ map, recorded with a ferromagnetically coated W tip at $U = -0.3$ V, $I = 0.3$ nA, and $T = 14$ K. Two types of 180° domain walls can be distinguished by their in-plane magnetization component (see arrows).

 

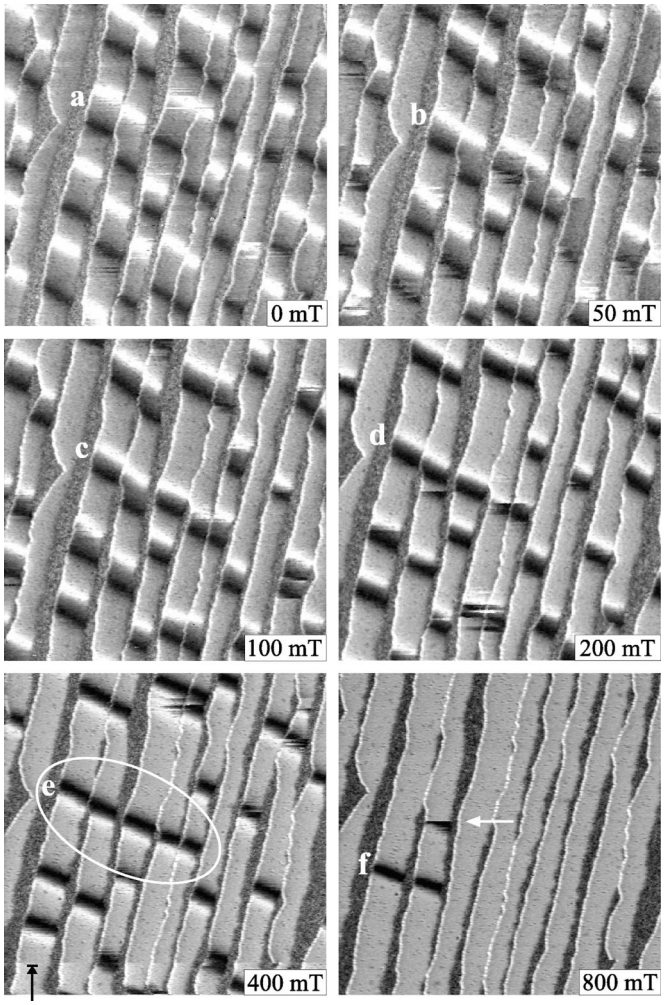


FIG. 2. $dI/dU$ maps of the surface area from Fig. 1, imaged in an increasing perpendicular magnetic field. Pairs of 180° domain walls are gradually forced together, which is equivalent to the formation and compression of 360° walls. At 800 mT, most of them have vanished (Ref. 8), i.e., the Fe film is in magnetic saturation. With increasing external magnetic field, the tip's magnetization is gradually forced from the in-plane towards the perpendicular direction.

DL wires that are separated by narrow regions of ML coverage, two types of 180° walls can be distinguished by their in-plane magnetization component (see arrows). They exhibit a wall width of $w \approx 7$ nm, in agreement with previous studies. The intermediate $dI/dU$ signal (gray) corresponds to a perpendicular magnetization oriented either up or down, two cases that cannot be distinguished with a tip exhibiting pure in-plane sensitivity, unless the symmetry is broken by an external field, as can be seen in the next figure.

Figure 2 shows $dI/dU$ maps of the same surface area in an increasing perpendicular magnetic field of up to 800 mT: Areas magnetized parallel to the field direction grow at the expense of antiparallel ones, and pairs of 180° walls are forced together, which is equivalent to the formation of 360° walls.[9] As expected, their lateral extension decreases with increasing field value.

A closer inspection of these field-dependent measurements reveals that (i) the magnetization rotates along every single nanowire with a defined chirality, and that (ii) the rotational sense is the same in each of the 12 wires within the imaged area. These findings are consistent with data from a previous publication[10] where in-plane and out-of-plane sensitivities were achieved with one and the same tip by choosing appropriate bias voltages $U$. Since the azimuthal angle of the tip magnetization is unknown, the absolute sense of rotation, however, cannot be determined. For the same reason it cannot be decided on the basis of these data alone whether the walls are of Bloch or Néel type, though the facts that the closed DL film is magnetized in plane along $[1\bar{1}0]$ at elevated temperatures[7] and the domain walls are oriented along the same direction[8] are an indication of their Bloch-type character. Observation (i) is already to be expected for stability reasons: neighboring walls of opposite chirality (unwinding or untwisted walls) attract each other and can easily annihilate, in contrast to winding walls. As a consequence, the cooling process of the sample from above $T_c$ to the measurement temperature of 14 K will result in a defined chirality within every individual wire, since such a structure is more stable against thermal fluctuations. The observed average distance between neighboring walls does therefore not necessarily reflect the magnetic ground state at low temperatures; since it might be a relict from the cooling process, which is effectively frozen in a metastable state. Observation (ii) is not yet fully understood. It might be connected to the miscut of the sample and/or the deviation of the axis of the wires from the [001] direction.

With increasing external magnetic field, the tip's magnetization is successively rotated from in-plane towards the perpendicular direction. Also its in-plane direction is reversed during data acquisition at 400 mT in Fig. 2 (see black arrow), which causes an inverted contrast for the remaining upper part of the image. At this field value a group of five 360° walls has formed a row (see oval), a correlation that might arise from their in-plane stray field. At 800 mT most of the 360° walls within the scanned area have been remagnetized by a rotation via the hard [001] in-plane direction.[2,3] It has been shown previously that in this process the stray field of the tip plays a significant role,[8] which can already be deduced from the fact that one of the remaining three walls disappears while it is imaged (see white arrow) and the other two remagnetize similarly during the repeated imaging at the same external field value (not shown). At lower field values the tip's stray field causes domain-wall movements that can be recognized by noncontinuous contrasts in the $dI/dU$ maps.

Note that at 800 mT the tip's magnetization $\vec{M}_T$ is close to the normal direction, resulting in an almost exclusive perpendicular sensitivity in this $dI/dU$ map, in contrast to the previous images. This issue is illustrated in Fig. 3 for a single 180° Bloch wall that is described by[4]

$$\varphi_{180}(x) = \arcsin\left(\tanh\left(\frac{x}{w_0/2}\right)\right), \quad w_0 = 2\sqrt{\frac{A}{K_{\text{eff}}}}. \qquad (1)$$

Since in SPSTM the variation of the $dI/dU$ signal is proportional to the projection of the local surface magnetization

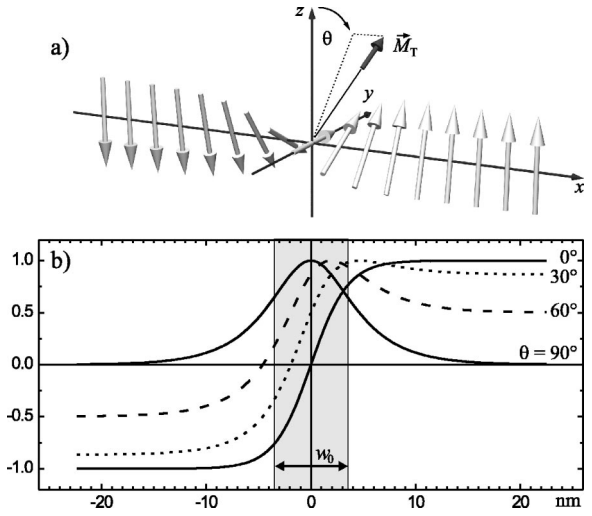


FIG. 3. (a) Schematic representation of a Bloch wall. (b) Wall profiles strongly depend on the tip's magnetization $\vec{M}_T$. The relevant angle $\theta$ is the one between the $z$ direction and the projection of $\vec{M}_T$ onto the $y$-$z$ plane.

onto the tip magnetization, measured wall profiles gradually change from pure domain-wall contrast at $\theta=90°$ to pure domain contrast at $\theta=0°$, where $\theta$ is the angle between the easy direction $z$ and the projection of $\vec{M}_T$ onto the wall plane $(yz)$.

We will now focus on the internal structure of the 360° walls. Figure 4 displays line sections (gray circles) of the single pair of domain walls, which have been shown in Fig. 2(a–f). We describe the wall profiles by the sum of two 180° walls at the positions $\pm c$:

$$\varphi_{360}(x)=\sum_{+,-}\arcsin\left(\tanh\left(\frac{x\pm c}{w/2}\right)\right). \tag{2}$$

The values of $c$ and $w$ can then be extracted from the data if the varying tip magnetization is taken into account. Using the function

$$y=y_0+a\cos(\varphi_{360}(x)+\theta), \tag{3}$$

the fitted curves (black lines) and the resulting fit parameters $\theta$, $c$, and $w$ are displayed within the figure. The extension of the inner 180° rotation between the two opposite in-plane orientations, which is approximately $2c$, has been marked by a shaded area. It successively decreases from 22.2 nm in zero field to 6.7 nm at 800 mT.

This compression of 360° walls observed in Fig. 4 can already be reproduced quantitatively within a simple 1D micromagnetic model, which takes into account Zeeman, exchange, and an effective anisotropy energy. The latter includes the crystal anisotropy and the local part of the dipolar energy. Nonlocal effects are neglected.[3] The total energy per unit area can then be written as

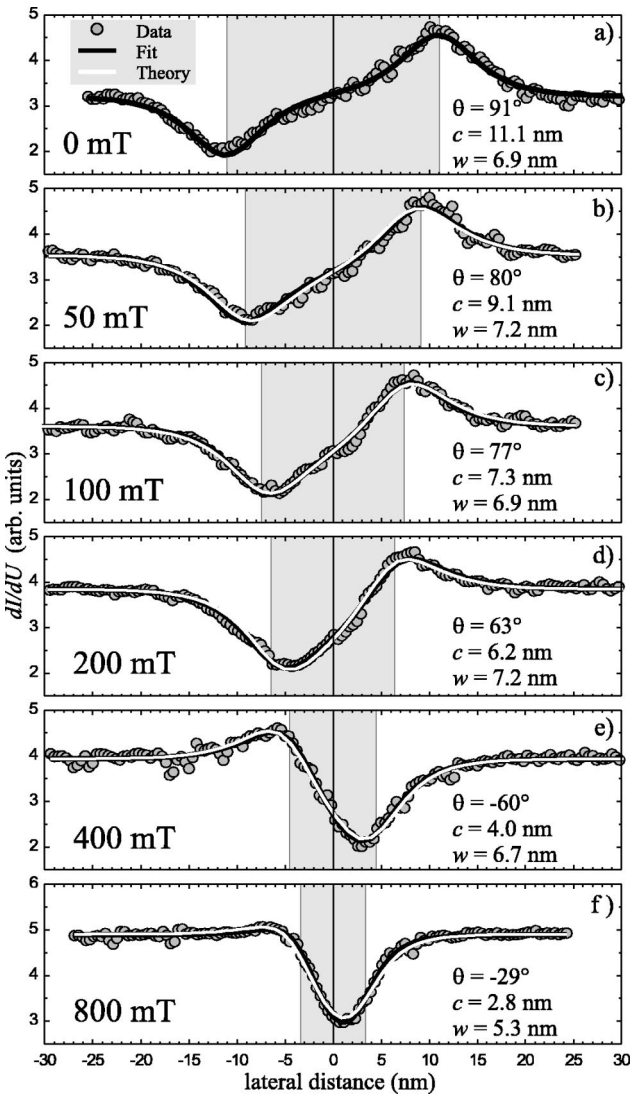


FIG. 4. Line sections (circles) across a single 360° wall corresponding to panels (a–f) in Fig. 2, as well as individual fits to the data (black lines) by Eq. (3) and expected profiles (white) using Eqs. (3) and (5). The shaded areas correspond to the walls' inner 180° spin rotation.

$$e=\int \underbrace{A\left(\frac{\partial\varphi}{\partial x}\right)^2}_{\text{exchange}}+\underbrace{K_{\text{eff}}\sin^2\varphi}_{\text{effective anisotropy}}+\underbrace{M_sB\cos\varphi}_{\text{Zeeman}}\,dx, \tag{4}$$

where $A$ is the exchange stiffness, $K_{\text{eff}}$ the effective anisotropy constant, and $M_s$ the saturation magnetization. Energy minimization with appropriate boundary conditions yields a surprisingly simple exact solution,[3] which has already been used in the fitting procedure, i.e. Eq. (2), where the field-dependent values of $c$ and $w$ are now given explicitly by

$$c=\frac{w}{2}\operatorname{arcsinh}\left(\sqrt{\frac{2K_{\text{eff}}}{M_sB}}\right),\quad w=2\sqrt{\frac{A}{K_{\text{eff}}+M_sB/2}}. \tag{5}$$

For $B\to 0$, the distance $2c$ diverges and the zero-field wall width $w_0$ from Eq. (1) is recovered. To compare this

model with the measured data, we have performed a simultaneous fit to all line sections under the constraint of Eqs. (5). Assuming a reasonable value of $M_s = 2.0 \times 10^6$ A/m, the other two magnetic constants are determined to $A = 1.82 \times 10^{-11}$ J/m and $K_{\text{eff}} = 1.25 \times 10^6$ J/m$^3$ in this procedure. The resulting curves are displayed as white lines in Fig. 4 and are in good agreement with the experimental data, even in the low-field regime. The only exception is the zero-field case. Here the equilibrium distance depends on the neighboring walls in the experiment and the theoretical model fails, since it considers a single-wall pair only. For $B \geqslant 50$ mT, however, the good agreement implies that indeed the compressing force arising from the Zeeman energy is balanced by an increasing energy penalty due to exchange alone. The dipolar energy contributes only indirectly to the 360° wall's extension, via a reduced effective anisotropy, which leads to an increased wall width $w$.

To verify this conclusion we performed additional calculations including a full description of the dipolar energy in a finite element approach.[11] We determined the equilibrium state for a single 360° wall in an isolated DL section of size $200 \times 20 \times 0.4$ nm$^3$. Since the dipolar energy is calculated explicitly, instead of $K_{\text{eff}}$ the crystal anisotropy alone had to be taken into account and was set to $K = 3.53 \times 10^6$ J/m$^3$ in order to reproduce $w_0$. For $B \geqslant 50$ mT, the results are indistinguishable from the ones obtained with the simple approach above, which means that nonlocal demagnetizing effects can be neglected in this field range. Only in external fields as small as a few mT, significant deviations are observed in the simulation, and the distance between the walls also depends on the sample's length.

## IV. CONCLUSION

Employing SPSTM we have investigated the internal structure of 360° walls in an increasing external field of $B = 50$–$800$ mT. At every field step their extension decreases and the equilibrium state is determined by a balance of exchange and Zeeman energy. It has been shown that nonlocal demagnetizing effects can be neglected in this field range, which means that the system exhibits a pure exchange repulsion of domain walls.

## ACKNOWLEDGMENTS

Financial support from the BMBF (Grant No. 13N7647) and from the DFG (Graduiertenkolleg ''Nanostrukturierte Festkörper'') is gratefully acknowledged.

*Email address: kubetzka@physnet.uni-hamburg.de

[1] X. Portier and A. Petford-Long, Appl. Phys. Lett. **76**, 754 (2000).
[2] E. Magyari and H. Thomas, Phys. Scr., T **44**, 55 (1992).
[3] H.-B. Braun, Phys. Rev. B **50**, 16 485 (1994).
[4] A. Hubert and R. Schäfer, *Magnetic Domains* (Spinger, Berlin, 1998).
[5] O. Pietzsch, A. Kubetzka, D. Haude, M. Bode, and R. Wiesendanger, Rev. Sci. Instrum. **71**, 424 (2000).
[6] O. Pietzsch, A. Kubetzka, M. Bode, and R. Wiesendanger, Phys. Rev. Lett. **84**, 5212 (2000).
[7] J. Hauschild, U. Gradmann, and H.J. Elmers, Appl. Phys. Lett. **72**, 3211 (1998).
[8] A. Kubetzka, M. Bode, O. Pietzsch, and R. Wiesendanger, Phys. Rev. Lett. **88**, 057201 (2002).
[9] O. Pietzsch, A. Kubetzka, M. Bode, and R. Wiesendanger, Science **292**, 2053 (2001).
[10] M. Bode, O. Pietzsch, A. Kubetzka, S. Heinze, and R. Wiesendanger, Phys. Rev. Lett. **86**, 2142 (2001).
[11] Object Oriented Micromagnetic Framework, OOMMF, Version 1.2 alpha 2 (http://math.nist.gov/oommf/).